Report

Current Biology

A pyritized Ordovician leanchoiliid arthropod

Highlights

- The youngest leanchoiliid arthropod described from the Late Ordovician of the USA
- Iron pyrite preservation allows high-resolution 3D reconstruction by CT scanning
- The head anatomy of leanchoiliids is resolved in unprecedented detail

Authors

Luke A. Parry, Derek E.G. Briggs, Ruixin Ran, Robert J. O'Flynn, Huijuan Mai, Elizabeth G. Clark, Yu Liu

Correspondence

luke.parry@earth.ox.ac.uk (L.A.P.), yu.liu@ynu.edu.cn (Y.L.)

In brief

Parry et al. describe a new leanchoiliid arthropod from the Ordovician Period that is preserved in pyrite, allowing it to be reconstructed in 3D, revealing new anatomical details. This group of arthropods is well known from the preceding Cambrian, but this new discovery reveals that they survived long after the Cambrian explosion.

Parry et al., 2024, Current Biology *34*, 1–9
December 2, 2024 © 2024 The Author(s). Published by Elsevier Inc.
https://doi.org/10.1016/j.cub.2024.10.013

CellPress

Please cite this article in press as: Parry et al., A pyritized Ordovician leanchoiliid arthropod, Current Biology (2024), https://doi.org/10.1016/j.cub.2024.10.013

Current Biology

CellPress
OPEN ACCESS

Report

A pyritized Ordovician leanchoiliid arthropod

Luke A. Parry,[1,8,*] Derek E.G. Briggs,[2,3] Ruixin Ran,[4,5] Robert J. O'Flynn,[4,5,6] Huijuan Mai,[4,5] Elizabeth G. Clark,[7] and Yu Liu[4,5,*]

[1]Department of Earth Sciences, University of Oxford, South Parks Road, Oxford OX1 3AN, UK
[2]Department of Earth and Planetary Sciences, Yale University, PO Box 208109, New Haven, CT 06520, USA
[3]Yale Peabody Museum, Yale University, New Haven, CT 06520, USA
[4]Yunnan Key Laboratory for Palaeobiology, Institute of Palaeontology, Yunnan University, 650500 Kunming, China
[5]MEC International Joint Laboratory for Palaeobiology and Palaeoenvironment, Yunnan University, 2 North Cuihu Road, Kunming 650091, China
[6]School of Geography, Geology and the Environment, University of Leicester, University Road, Leicester LE1 7RH, UK
[7]Advanced Light Source, Lawrence Berkeley National Laboratory, Berkeley, CA, USA
[8]Lead contact
*Correspondence: luke.parry@earth.ox.ac.uk (L.A.P.), yu.liu@ynu.edu.cn (Y.L.)
https://doi.org/10.1016/j.cub.2024.10.013

SUMMARY

The "short-great-appendage" arthropods (Megacheira), such as *Leanchoilia*, have featured heavily in discussions of arthropod evolution, particularly related to the head and its appendages.[1–4] Megacheirans are subject to competing interpretations, either as a clade[4] or a grade,[5] in the stem group of Euarthropoda[6] or, alternatively, Chelicerata.[4] They are most diverse in Cambrian Burgess-Shale-type deposits, where the family Leanchoiliidae is represented by six genera,[7–12] characterized by the presence of three distal flagella on the great appendage with a presumed sensory function. We describe the first post-Cambrian member of this family, *Lomankus edgecombei* gen. et sp. nov, from the Upper Ordovician (Katian) Beecher's Trilobite Bed site of New York State—the first post-Cambrian megacheiran with the exception of the Silurian and Devonian Enaliktidae. Micro-computed tomography (micro-CT) scanning reveals the morphology of the short great appendage with elongate flagella, four biramous cephalic limbs, 11 trunk segments with biramous limbs and dorsal tergites, and an elongate telson unique within Leanchoiliidae. The great appendage is also unique: the long endites that bear the flagella in other leanchoiliids are absent (or at least greatly reduced) and each flagellum appears to attach directly to an individual podomere, suggesting a sensory rather than a raptorial function. The remarkable preservation of a well-developed ventral plate (epistome-labrum complex) anterior of the mouth reinforces a deutocerebral origin[2,13] of the short great appendages. *Lomankus edgecombei* unveils the three-dimensional (3D) head morphology of leanchoiliids in unparalleled detail and demonstrates that these iconic fossil arthropods ranged into dysaerobic environments in the Ordovician, where *Lomankus* occupied a deposit-feeding niche.

RESULTS

Systematic paleontology

Phylum Euarthropoda Lankester,[14]
Class Megacheira Hou and Bergström,[15]
Order Leanchoiliida Størmer,[16]
Family Leanchoiliidae Raymond,[17]
Genus *Lomankus* gen. nov.

Etymology

From the Greek *loma* (edge, border) and *ankos* (valley), derived from the meaning of Edgecombe, edge of a valley.

Diagnosis

As for the species (by monotypy).

Lomankus edgecombei sp. nov.

Holotype

YPM IP 256612 (Figures 1A and 2C–2H).

Paratypes

YPM IP 256613 (Figures 1B, 2A, and 2B), YPM IP 236743 (Figures 1C and 2I–2M), YPM IP 516237 (Figures 1D and 1E), and YPM IP 236744 (Figure 1F).

Etymology

For Gregory D. Edgecombe, in recognition of his contributions to our understanding of arthropod evolution.

Diagnosis

Cephalic region with short great appendage and four biramous appendages. Endites of short great appendage absent or reduced, such that flagella attach directly to individual podomeres. Head appendages two and three smaller than successive limbs, with multisegmented exopods that resemble the endopods. Head appendages four and five similar to those of the trunk, which consist of endopods with five podomeres plus a terminal claw, flap-like exopod, and exite. Well-developed ventral

This is an open access article under the CC BY license (http://creativecommons.org/licenses/by/4.0/).

Please cite this article in press as: Parry et al., A pyritized Ordovician leanchoiliid arthropod, Current Biology (2024), https://doi.org/10.1016/j.cub.2024.10.013

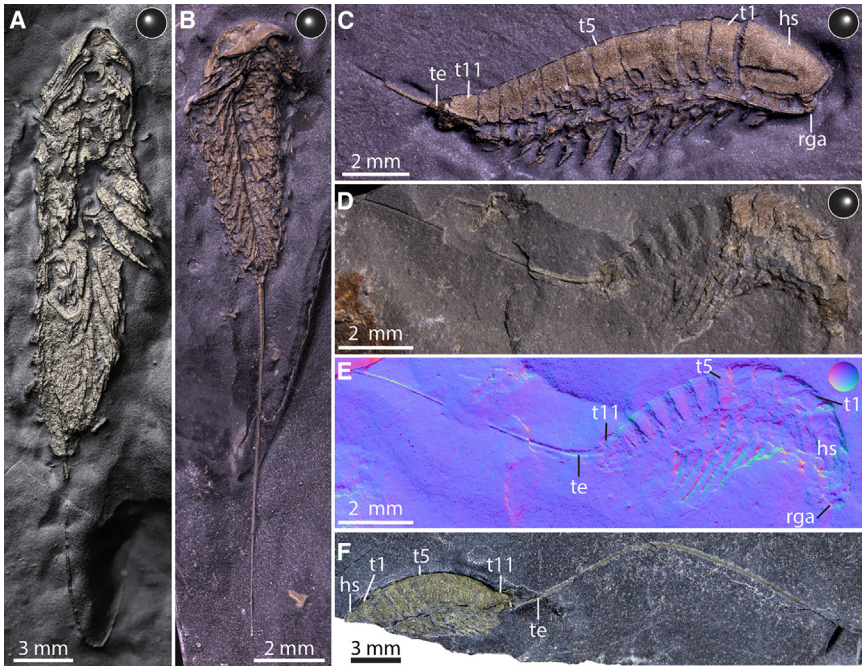

Figure 1. *Lomankus edgecombei* from the Beecher's Trilobite Bed site of New York State

(A) Ventral view, YPM IP 256612, RTI image using normal unsharp masking.

(B) Ventral view, YPM IP 256613, RTI image using diffuse gain.

(C) Right lateral view, YPM IP 236743, RTI image using diffuse gain.

(D) Right lateral view, partially exposed, YPM IP 516237, RTI image using diffuse gain. See Figure S1 for illustration of the counterpart.

(E) Normal visualization reflectance transformation image showing tergites and trunk limbs, YPM IP 516237.

(F) Left lateral view, incomplete anteriorly, YPM IP236744. hs, headshield; lga, left great appendage; rga, right great appendage; tn, tergite number n; te, telson.

plate anterior and ventral of the mouth opening. Eyes absent. Telson with triangular proximal portion lacking fringing spines and extending into a long flagelliform termination.

Life Science Identifier (LSID)

Zoobank LSID: urn:lsid:zoobank.org:pub:61DCBEAA-6402-4A73-A6C9-6B18D2A227AD.

Locality

The specimens were collected in the vicinity of the original Beecher's Trilobite Bed site adjacent to Six Mile Creek near Rome in the Frankfort Shale of central New York State (Upper Ordovician, Katian Stage). YPM IP 256612 and YPM IP 256613 were collected from a level above the 2-m section that includes the original Beecher's Trilobite Bed. YPM IP 236743 was found about 50 m downstream of the Walcott Quarry and YPM IP 516237 an unspecified distance upstream of the Walcott Quarry, both at levels of unknown equivalence to those in Farrell et al.[18]

Preservation

The specimens were captured by rapid sedimentation events caused by turbidity currents. An unusual combination of factors, including rapid burial in sediments with high concentrations of sulfate and reactive iron led to pyritization of soft tissues.[19,20] YPM IP 256612 and YPM IP 256613 are exposed in ventral view (Figures 1A and 2A), whereas the remaining three are exposed in right (Figures 1C and 1D) or left (Figure 1F) lateral view. Only one of the specimens in lateral view is complete (Figure 1C); the others are effaced, with partial retention of the pyrite on the part and counterpart (Figures 1D and 1E) or missing the anterior (Figure 1F).

Description

General form. The elongate body of this small arthropod (~8–20 mm exclusive of the telson) is differentiated into head, segmented trunk, and non-somitic telson (Figures 1 and 2). The 17 segments comprise an ocular (but without evidence of eyes) and 16 post-ocular appendage-bearing segments (Figures 1A–1D, 2A–2D, 2I, and 2J). The ocular segment and post-ocular segments 1–5 are incorporated into the head, their dorsal area contributing to the head shield (Figure 3). Segments 6–16 form a trunk with dorsal tergites (Figures 1A–1D).

Head. The head shield is sub-triangular in dorsal view, narrowing near the anterior extremity, its length similar to the width at the posterior margin (Figure 2D). The axial region is poorly defined although the anterior rim is raised medially.

Eyes. There is no evidence of eyes. The space where eyes might be present (presumably the ocular segment/anterior sclerite) is unoccupied (Figures 3D–3F).

Ventral plate. There is an elongate structure with an oval outline (Figures 3B–3F) on the ventral side of the head, slightly posterior of the insertion of the great appendages. The mouth opening presumably lies posterior of this structure, based on the topological relationships between this feature and other anatomical features (e.g., great appendages). We refer to this structure as the epistome-labrum complex below (see discussion for details).

Head appendages. Head appendage one, the great appendage, originates at the antero-lateral margin of the epistome-labrum complex. It is differentiated into a peduncle and distal flagella-bearing portion (Figures 2E, 2K, and 3J–3L), separated by an elbow joint. The peduncle consists of two elements (Figures 3J–3L), which are slightly shorter than wide (diameter). Three long, slender flagella (Figures 2E and 2K) originate directly on the distal portion of the appendage, not on elongate endites projecting from these podomeres as in *L. superlata*, and project postero-laterally more than 50% of the body length (head and trunk) excluding the telson spine, i.e., as far as the fifth or sixth trunk tergite (Figure 2D). The first flagellum-bearing podomere is the most massive, shorter than wide (diameter). The second is much shorter, and the third (most distal) flagellum-bearing segment is much shorter and narrower, with a flagellum similar to the others (Figures 2E, 2K, 3K, and 3L).

Please cite this article in press as: Parry et al., A pyritized Ordovician leanchoiliid arthropod, Current Biology (2024), https://doi.org/10.1016/j.cub.2024.10.013

CellPress
OPEN ACCESS

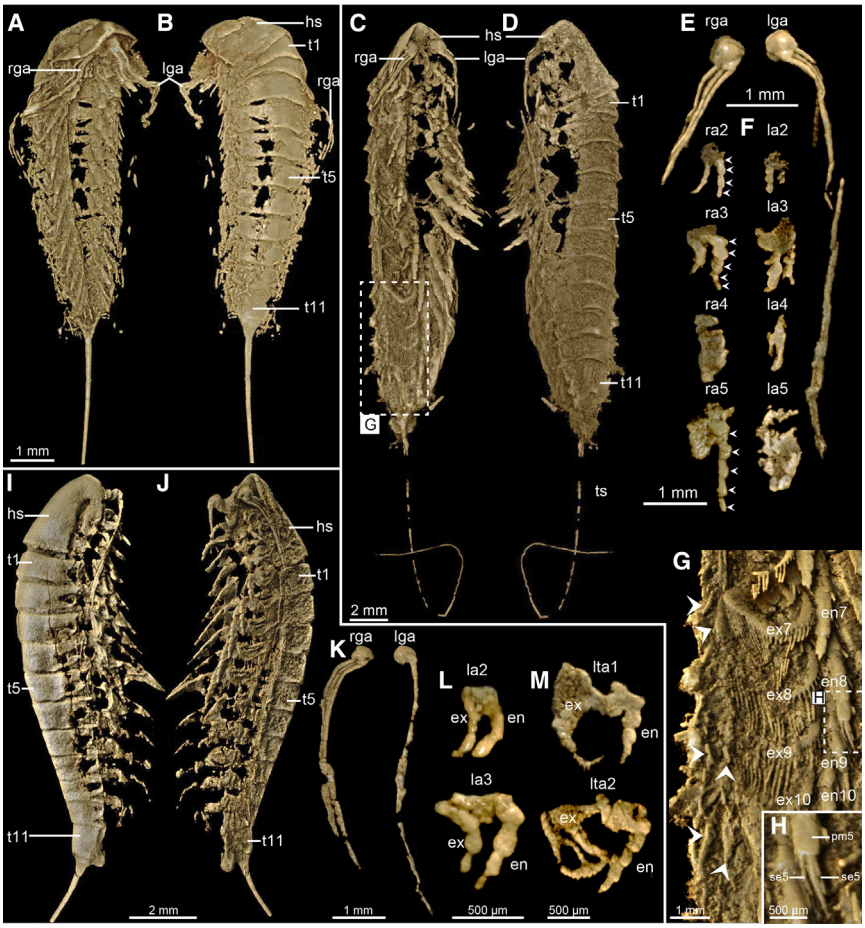

Figure 2. Morphology of *Lomankus edgecombei* reconstructed using computed tomography

(A and B) YPM IP 256613. (A) Ventral and (B) dorsal view.

(C–G) YPM IP 256612. (C) Ventral and (D) dorsal view; (E) great appendages; (F) head appendages 2–5; (G) posterior trunk appendages—boxed region in (C) shows location.

(H) Close-up of the terminal claw and flanking setae of endopod 9.

(I–M) YPM IP 236743. (I) Dorsolateral and (J) ventrolateral view; (K) great appendages; (L) left head appendages 2 and 3; (M) trunk appendages 1 and 2. en, endopod; ex, exopod; hs, headshield; lga, left great appendage; lta, left trunk appendage; rga, right great appendage; se, terminal setae; pm, podomere; tn, tergite number n; ts, telson. Arrowheads in (G) identify the position of exites. See also Figure S1.

Head appendages two and three are smaller than the more posterior appendages (Figures 2F and 2L). They consist of a basipod (in some cases obscured by pyrite) and two rami. The endopod of appendage two consists of four podomeres (Figure 2F), the first shorter and wider (diameter) than the others. Podomeres two and three are similar in length and four is narrower than the others. The other ramus (presumably exopod) is similar to the endopod but more slender with shorter podomeres, greater in number than in the endopod. Appendage three is a little larger than appendage two (Figures 2F and 2L). The endopod consists of at least five podomeres, the distal ones longer than wide (Figures 2F and 2L), the appendage tapering distally. The exopod is similar to the endopod but smaller with fewer podomeres. There were likely setae on the rami of appendages two and three but they were not captured by pyritization.

Head appendage four is similar in size or slightly larger than appendage three (Figure 2F). The morphology is obscured by incomplete or overgrown pyritization, but there is possible evidence of a flap-like exopod (Figure 2F). Head appendage five, the posteriormost head appendage, is larger than appendage four but likewise obscured by pyritization (Figure 2F). The endopod consists of at least five podomeres, one and two shorter than the others, three and four expanding individually to their midlength or just beyond, and element five narrower (Figure 2F). The exopod is obscured, but the right side of YPM IP 256613 preserves the distal part of the somewhat flattened endopod and a curved remnant with evenly spaced projections (Figures 2I and 2J) (also possibly present on appendage four), which may represent the thickened margin of a flap-like exopod with projecting setae similar to those on the rest of the trunk (Figures 2C and 2G). Thus, the posterior two head appendages may be similar to those of the trunk.

Trunk. The first two or three trunk tergites are similar in width or a little wider than the head shield; the trunk tapers very gradually posteriorly beyond this point (Figures 2A and 2D). The trunk tergites are about one-third the length of the head shield, reducing slightly only in the last few (Figures 2I and 6J). There is no strongly developed pleural region nor is there evidence of serrations on the lateral rim of the tergites (Figures 1C and 2I).

Trunk appendages. The anterior trunk appendages are larger than the posterior head appendages (Figures 2L and 2M). The detail of appendages preserved along the length of the trunk is variable, a reflection of pyritization as well as preparation before we acquired the specimens (Figures 2I, 2M, and 2G). However, the combined evidence of YPM IP 236743, 256612, and 256613 shows that the appendages were similar throughout (Figures 2A, 2C, 2I, and 2J), apart from decreasing in size gradually beyond trunk appendage four. The endopods consist of five podomeres plus a terminal curved claw (Figure 2G). Spines/setae project from the podomeres, where they articulate with the next most distal podomere. Two elongate spines on the fifth podomere flank the terminal claw laterally (Figure 2H). The exopods overlap and are suboval in shape, with a thickened margin fringed by multiple long setae, perhaps as many as 30 (Figure 2G).

Lamellar outgrowths that presumably emerge from the protopodite are evident in the trunk appendages of segments seven, nine, and ten in YPM IP 256612. At least two lamellae are present, with an exposed length extending about 25% the length of the corresponding endopods (Figure 2G). These features are

Please cite this article in press as: Parry et al., A pyritized Ordovician leanchoiliid arthropod, Current Biology (2024), https://doi.org/10.1016/j.cub.2024.10.013

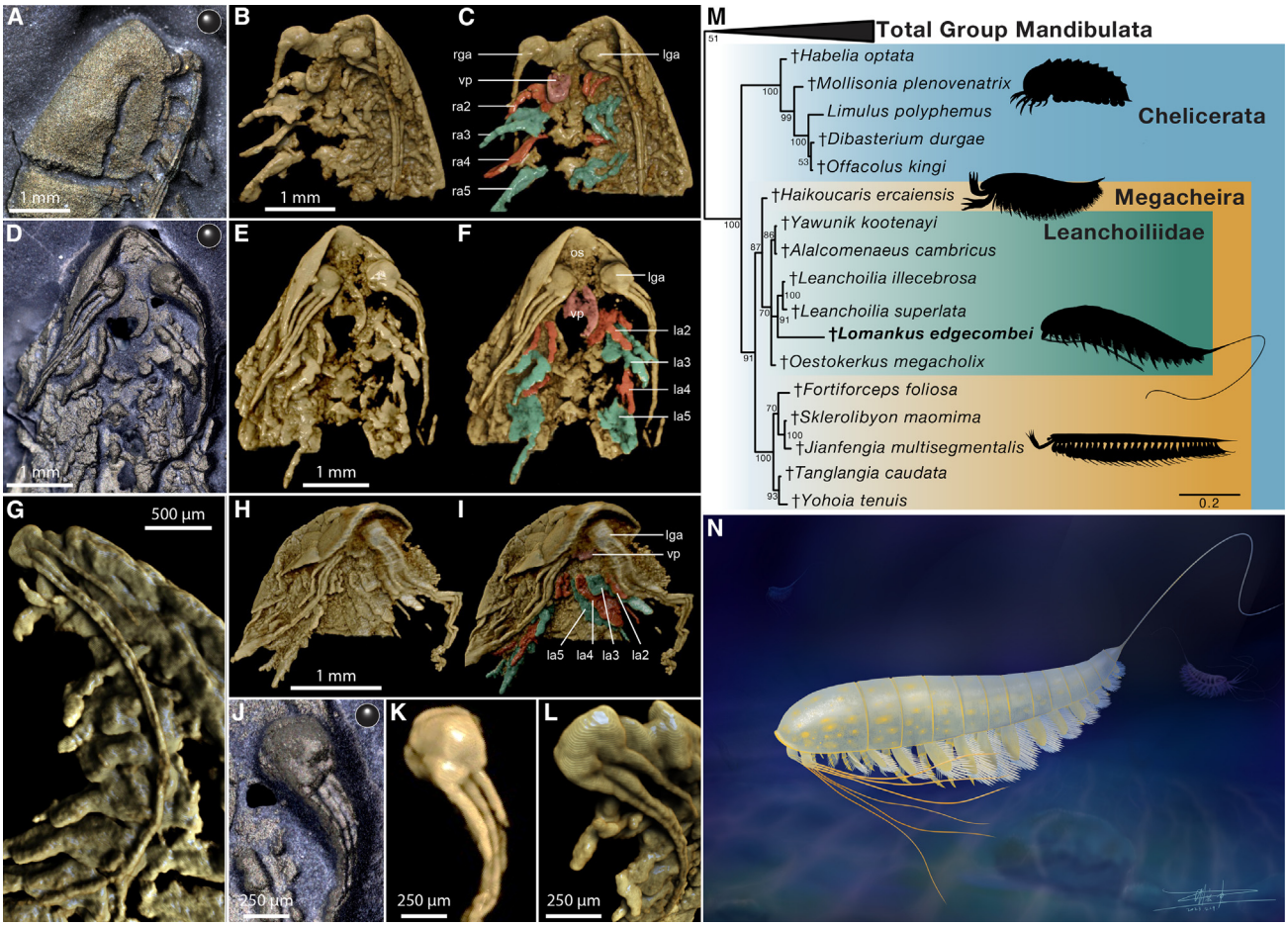

Figure 3. Morphology of the head region and great appendage of *Lomankus edgecombei*, phylogeny, and life reconstruction

(A–C) YPM IP 236743. (A) Right lateral view, RTI image using diffuse gain rendering; (B and C) CT reconstruction, ventrolateral view.

(D–F) YPM IP 256612. (D) Ventral view, RTI image using diffuse gain rendering; (E and F), CT reconstruction, ventral view.

(G) YPM IP 516237, CT reconstruction, left lateral view.

(H and I) YPM IP 256613, ventral view.

(J and K) YPM IP 256612, great appendage. (J) Ventral view of great appendage, RTI image using diffuse gain rendering; (K) CT reconstruction of great appendage, ventral view.

(L) YPM IP 516237, CT reconstruction of great appendage, left lateral view.

(M) Bayesian phylogeny based on a morphological dataset of 283 characters and 87 taxa. Majority rules consensus tree of analysis performed under the mki + gamma model using MrBayes 3.2.7. Numbers at nodes are posterior probabilities and branch lengths, and scale bars are in units of expected number of substitutions per site. Silhouettes from Phylopic (see acknowledgments for credits) except for *Lomankus edgecombei* by L.A. Parry.

(N) Life reconstruction of *Lomankus edgecombei* by Xiaodong Wang. lan, left appendage n; lga, left great appendage; os, ocular sclerite; ran, right appendage n; rga, right great appendage; vp, ventral plate.

See also Figures S2 and S3.

interpreted as exites[21] and, therefore, must be considerably longer in order to attach to the corresponding basipods.

Telson. The telson is elongate triangular in dorsal view (Figure 2B), extending into a long, gradually tapering, flexible spine that exceeds the length of the body (Figures 1, 2C, and 2D).

Phylogenetic analysis

Our phylogenetic analyses recover *Lomankus edgecombei* as a member of Megacheira (Figure 3M). Maximum parsimony analyses recover *L. edgecombei* in a relatively deep position within the class, either as the sister taxon of Megacheira (equal weighting; Figure S2A) or of the rest of the total group of Chelicerata (implied weighting; Figure S2B). Parsimony character state optimizations infer that shared derived characters of the family Leanchoiliidae originate convergently in *L. edgecombei* (Figure S2). The absence of typical leanchoiliid characters (e.g., spinose endites of the great appendages) are primary absences. Support values for the placement of *L. edgecombei* are generally low.

Bayesian analyses, in contrast, recover *L. edgecombei* as the sister taxon of the genus *Leanchoilia*, at the tip of a branch that has a root-to-tip distance greater than that of all other megacheirans, consistent with the accumulation of additional character state changes during the ~60 million years separating it from Cambrian megacheirans. This observation, together with

Please cite this article in press as: Parry et al., A pyritized Ordovician leanchoiliid arthropod, Current Biology (2024), https://doi.org/10.1016/j.cub.2024.10.013

CellPress
OPEN ACCESS

simulation studies[22] that suggest that the results of Bayesian analyses of datasets with large proportions of fossil tips are more accurate than maximum parsimony analyses, prompt us to favor the Bayesian results as a basis for the taxonomic assignment of *L. edgecombei*.

DISCUSSION

The rare settings where early pyritization leads to exceptional preservation provide a more complete picture of diversity than the normal shelly fossil record; other notable examples include the Cambrian Stage 3 Chengjiang Biota[23] and the Devonian Emsian Hunsrück Slate.[24] This is particularly important in Paleozoic sequences, where early representatives of taxa may reveal morphological character state combinations that were subsequently lost through extinction.[25,26]

Beecher's Trilobite Bed is renowned as the site where trilobites preserving limbs were first discovered in the 1890s. C.E. Beecher of Yale University quarried the site in 1893 and described the pyritized appendages of the olenid *Triarthrus* in a number of papers (see Whittington and Almond[27]). Restudies of the appendages employed X-radiography[28,29] or classic techniques,[27] and *Triarthrus* remains one of the most completely known trilobites.[30] Beecher's original Trilobite Bed and adjacent horizons preserving pyritized fossils were deposited from turbidite events. The faunal content of the interbedded silty claystone background beds is similar, indicating that the sequence samples a local community.[20] The evidence of sediment geochemistry and trace fossils, in addition to the nature of the fauna, reflects low oxygen dysaerobic conditions.[18,20] The assemblages at different levels in the section that includes the original Trilobite Bed differ in the taxa present and their proportions. Overall, however, the low-diversity fauna is dominated by the trilobite *Triarthrus* and includes rarer trilobites, ostracods, and brachiopods as well as orthocone nautiloids and graptolites introduced from the water column.[20] The discovery of other arthropods such as *L. edgecombei* beyond the Beecher's Trilobite Bed section indicates a greater diversity of non-biomineralized taxa, but their preservation in pyrite is evidence of similar low oxygen conditions.

The majority of Leanchoiliidae are known from the Cambrian Series 2 and the Miaolingian[9,15,31]: *L. edgecombei* is the first Ordovician representative of the clade, extending the stratigraphic range of this clade of iconic arthropods beyond Cambrian Burgess-Shale-type deposits.[9,31–33] It echoes the discovery of other typical Burgess-Shale-type panarthropods, including lobopodians, radiodonts, and marrellomorphs, in the Lower Ordovician Fezouata formations of Morocco.[34] Such discoveries emphasize the importance of appropriate taphonomic conditions, such as those associated with Beecher's Trilobite Bed, in extending the temporal and spatial range of non-biomineralized arthropods and providing important evidence of the early evolution of this, the most diverse clade of invertebrates.

Two unusual short-great-appendage arthropods are known from later Paleozoic strata, *Enalikter aphson* from the Silurian Herefordshire Lagerstätte and *Bundenbachiellus giganteus* from the Devonian Hunsrück Slate,[5] and are assigned to a second family of Leanchoiliida, Enaliktidae. Enaliktidae is characterized by a short head with just three appendages. The great appendage lacks a geniculum, the three flagella originate closely rather than on distinct podomeres, drawing a comparison with the antennule of some decapod crustaceans,[35] and the trunk divisions lack paratergal folds and bear appendages with fan-like exopods. The unusual morphology of *E. aphson* even led some to argue that its affinity lies with polychaetes,[36] although this has been strongly disputed.[37,38] Due to uncertainties about details of morphological characters in *E. aphson* and *B. giganteus*, Aria et al.[12] omitted them from their analysis of the affinities of the leanchoiliid *Yawunik kootenayi* from the Marble Canyon locality of the Burgess Shale. Here, we likewise focused on determining the place of *L. edgecombei* among its familiar Cambrian representatives within the family Leanchoiliidae.

The differentiated head region with five appendages, deutocerebral short great appendage with three flagella, and eleven post-cephalic tergites identify *L. edgecombei* as a member of Leanchoiliidae.[31,39] The flagella of the great appendage appear to attach directly to podomeres, indicating that endites, which are elongate in other members of the family, are absent or reduced in *L. edgecombei* such that they cannot be distinguished from the proximal part of the flagellum. This short great appendage morphology is unique among Leanchoiliidae and Megacheira. The small triangular telson in *L. edgecombei* extends into a long, flexible flagellum-like feature, unlike the triangular telson fringed with spines[33] that is typical of Cambrian megacheirans. These two major anatomical differences justify the erection of a new genus. The great appendage of *L. edgecombei* differs from that of *Leanchoilia superlata* in that the terminal claw[12]/C4[31] is absent. Although this terminal claw is present as a hooked spine in adult *Leanchoilia illecebrosa* (but absent in its larvae[40]) and in some other members of Leanchoiliidae, such as *Yawunik kootenayi*,[12] it is not a feature of the leanchoiliid *Oestokerkus megacholix*[9] or other megacheirans, such as Jianfengiidae[41] or the putative megacheiran *E. aphson*.[12] The trunk appendages resemble those of *L. illecebrosa* in the presence of exites[21] and the morphology of the terminal claw and setae on the final podomere. However, the appendages differ in the number of podomeres: five in *L. edgecombei* versus eight in *L. illecebrosa*. Exites have not been reported in *L. superlata* from the Burgess Shale despite extensive study of this species.[31] However, they may not be evident due to their small size or concealment beneath other anatomical features (e.g., tergites). Exites were identified in *L. illecebrosa* only following computed tomography (CT) scanning. Consequently, we code this feature as uncertain rather than absent in *L. superlata*.

The head shield of *L. edgecombei* (Figures 2A, 2C, 3A–3F, 3H, and 3I) lacks an anterior hook-like structure similar to that in *L. superlata* or a pointed termination as in *L. illecebrosa*. Nor is there evidence of serrations on the rim of the head shield (Figures 2A, 2C, 3A–3F, 3H, and 3I) or carinae in the posterior region of head shield or trunk tergites (Figures 2B, 2D, and 2I), in contrast to *L. superlata*. *L. edgecombei* lacks evidence of eyes, in contrast to *L. superlata* and *L. illecebrosa*, where two pairs of eyes lie anterior of the labrum and great appendages.[2,12] Pyritization of other features of *L. edgecombei* makes it unlikely that eyes were lost via decay prior to mineralization; eyes are clearly preserved in pyritized specimens of

Please cite this article in press as: Parry et al., A pyritized Ordovician leanchoiliid arthropod, Current Biology (2024), https://doi.org/10.1016/j.cub.2024.10.013

L. illecebrosa from Chengjiang,[2] showing that leanchoiliid eyes are susceptible to mineralization in deposits with similar pyritization of soft tissues. Although complete loss of eyes is relatively rare in euarthropods, *Lomankus* co-occurs with the blind trinucleid trilobite *Cryptolithus*,[42] indicating the presence of at least one other blind euarthropod in assemblages known from Beecher's Bed fossil sites.

L. edgecombei differs from *Leanchoilia* in the lack of evidence for eyes, presence of numerous long setae fringing the exopods, and the flagella-like projection of the telson. Among megacheirans, such an elongate telson morphology is known only in *Tanglangia longicaudata*.[43] The great appendage differs in the shorter peduncle, lack of elongate endites bearing the flagella, and greater tendency to project backward beneath the trunk rather than forward. These differences presumably reflect a contrasting mode of life, perhaps associated with non-visual foraging on the benthos, with the great appendages performing a sensory rather than raptorial function.

The structure of the head and identity of the segment bearing the great appendages of leanchoiliids and other megacheirans have featured in the debate about the "arthropod head problem."[1,2,13,44] Recent work has established a six-segmented head as plesiomorphic for megacheirans, consisting of an ocular segment and those bearing the great appendage and four pairs of biramous limbs.[2,32] Fewer biramous limbs are known in *L. superlata* from the Burgess Shale,[31] which is either a derived condition or indicates that a very small first biramous appendage was not detected.[32] The first biramous limb in *L. illecebrosa* was only revealed by micro-CT scanning.[2] The segmental identity of the great appendage and its homology with anterior appendages of other panarthropods has been a source of controversy, with competing interpretations favoring either a protocerebral[1,45] or deutocerebral[3,46,47] affinity, the latter arguing homology between the great appendage and the antennule of crustaceans and the chelicera of chelicerates.[47] This dichotomy was apparently resolved through the discovery of a reduced, paired labrum (equivalent to the epistome-labrum complex here, with associated structures that are protocerebral or pre-segmental in origin and present in all extant euarthropods except pycnogonids[44,48]) in juveniles of *L. illecebrosa*,[2] affirming a deutocerebral identity for the great appendage. Budd,[1] however, argued that the structure identified by Liu et al.[2] was a more diffuse "epistome," invoking a comparison with *Fuxianhuia*.[49]

More recent investigations of the megacheirans *Jianfengia*[32] and *Tanglangia*[43] identified a lobate ventral plate anterior of the mouth, but we report the first unambiguous evidence (see Haug et al.[31] for a possible hypostome in *L. superlata*) of a ventral plate in the adult form of Leanchoiliidae, demonstrating its presence across the diversity of Megacheira. In extant euarthropods, there is a corresponding sclerotization anterior of the labrum (the clypeus/epistome) that accommodates the insertion of the anteriormost pair of appendages.[50,51] Uncertainty regarding the identification of the labrum in fossil taxa has resulted in them being referred to as a single anatomical unit in paleontological papers (commonly referred to as the hypostome-labrum complex[32,51–53]). In trilobites, this distinction was apparently resolved through study of exceptionally preserved specimens entombed in volcanic ash,[51] where the labrum was identified as a distinct structure that is attached to the posterior of the hypostome. That study revealed that the hypostome supported the insertion of the trilobite antenna, resulting in topological relationships between the hypostome, labrum, and anteriormost appendages that closely correspond to the epistome, labrum, and chelicera (e.g., in *Limulus*[50]), respectively, in chelicerates, further supporting the inference that these features are homologous across euarthropods (although for an alternative view of the trilobite hypostome, see Park[53]). Given this morphological resemblance and the inferred chelicerate affinity of Megacheira (e.g., Figure 3M), we refer to the ventral plate identified in *Lomankus* as the epistome-labrum complex.

A ventral sclerotization anterior of the mouth (clypeus/epistome/hypostome), in combination with the presence of the labrum, is widely regarded as a synapomorphy of Euarthropoda.[2] The presence of these features is typically interpreted as incompatible with a protocerebral origin for the anterior appendage, i.e., the short great appendage in the case of megacheirans. Although we are unable to identify the labrum itself in *L. edgecombei*, the epistome-labrum complex supports the insertion of the great appendages (e.g., Figures 3A–3F), just as the hypostome supports the trilobite antenna (i.e., via the antennal notch). The topological relationships of features of the head of *Lomankus* therefore closely correspond to those in crown-group euarthropods with a deutocerebral first appendage and, as in the case of trilobites, the relationship between the appendage and hypostome matches that between the chelicera and epistome of *Limulus*.[50] The presence of a epistome-labrum complex in multiple megacheiran lineages is consistent with affinities close to or within the arthropod crown group, as recovered in our phylogenetic analysis (e.g., Figure 3M), and is consistent with evidence from juveniles of *L. illecebrosa*[2] and neuroanatomical evidence.[3] In *L. illecebrosa*, the epistome-labrum complex is relatively indistinct,[2] becoming less conspicuous through ontogeny, whereas in *Lomankus* and other megacheirans[32,43] it was well developed, suggesting that it was characteristic of the megacheiran ancestor.

The discovery of *L. edgecombei* demonstrates that leanchoiliids, an iconic clade of Cambrian arthropods, survived through the Ordovician. The modification of the first appendage in *L. edgecombei* demonstrates that they continued to innovate beyond the Cambrian, with the eponymous great appendage transitioning from a raptorial to sensory function, most likely in concert with a change from a predatory mode of life, mirroring similar transitions in other groups of Cambrian apex predators.[54–56]

RESOURCE AVAILABILITY

Lead contact

Further information and requests for resources should be directed to and will be fulfilled by the lead contact, Luke Parry (luke.parry@earth.ox.ac.uk).

Materials availability

All specimens of *Lomankus edgecombei* are deposited at the Yale Peabody Museum, with the following YPM IP accession numbers: YPM IP 256612, YPM IP 256613, YPM IP 236743, YPM IP 516237, and YPM IP 236744.

Data and code availability

The tiff stacks from CT scanning used to render the 3D reconstructions, the reflectance transformation datasets, and the morphological character matrix are available from the Oxford University Research Archive: http://dx.doi.org/10.5287/ora-mnjxxmoyd.

Please cite this article in press as: Parry et al., A pyritized Ordovician leanchoiliid arthropod, Current Biology (2024), https://doi.org/10.1016/j.cub.2024.10.013

CellPress
OPEN ACCESS

ACKNOWLEDGMENTS

Markus Martin provided information on the source of the specimens. We thank Mr Xiaodong Wang (Kunming) for providing the reconstruction and Greg Edgecombe for helpful comments on an earlier version of this manuscript and discussions of arthropod anatomy. This study was supported by an NERC independent research fellowship to L.A.P. (NE/W007878/1) and by a grant from the Natural Science Foundation of Yunnan Province (202301AS070049) to Y.L., who is further supported by the Yunnan Revitalization Talent Support Program. L.A.P. thanks the Yale Institute for Biospheric Studies for supporting a postdoctoral fellowship during which this work initiated. We thank Mr. Zhiliang Tian for the donation of two of the studied specimens. We thank the Willi Hennig Society for the use of TNT. Silhouette images in Figure 3M were sourced from Phylopic. *Mollisonia plenovenatrix* was created by Junnn11 (CC-BY-SA-3.0), *Haikoucaris ercaiensis* was created by Junnn11 and modified by T.-Michael-Keesey (CC-BY-NC-SA-3.0), *Fortiforceps foliosa* was created by Ghedoghedo and vectorized by T.-Michael-Keesey (CC-BY-SA-3.0), and *Jianfengia multisegmentalis* was created by Dinghua-Yang (modified by T.-Michael-Keesey [CC-BY-4.0]).

AUTHOR CONTRIBUTIONS

D.E.G.B., Y.L., and L.A.P. conceived the project. L.A.P. wrote the initial manuscript, with subsequent input from D.E.G.B. and Y.L. All authors approved the final manuscript. D.E.G.B. wrote the initial description, with subsequent input from L.A.P. and Y.L. R.R. and Y.L. rendered the CT data and produced the 3D models. R.J.O'F., D.E.G.B., and L.A.P. coded the phylogenetic character matrix and performed the phylogenetic analyses. H.M., E.G.C., and L.A.P. scanned the specimens. L.A.P. made the figures and produced the RTI datasets.

DECLARATION OF INTERESTS

The authors declare no competing interests.

STAR★METHODS

Detailed methods are provided in the online version of this paper and include the following:

- KEY RESOURCES TABLE
- EXPERIMENTAL MODEL AND STUDY PARTICIPANT DETAILS
  - Fossil specimens
- METHOD DETAILS
  - Reflectance transformation imaging
  - CT scanning and reconstruction
- QUANTIFICATION AND STATISTICAL ANALYSIS
  - Phylogenetic analysis

SUPPLEMENTAL INFORMATION

Supplemental information can be found online at https://doi.org/10.1016/j.cub.2024.10.013.

Received: June 28, 2024
Revised: August 16, 2024
Accepted: October 2, 2024
Published: October 29, 2024

REFERENCES

1. Budd, G.E. (2021). The origin and evolution of the euarthropod labrum. Arthropod Struct. Dev. *62*, 101048. https://doi.org/10.1016/j.asd.2021.101048.
2. Liu, Y., Ortega-Hernández, J., Zhai, D., and Hou, X. (2020). A reduced labrum in a Cambrian great-appendage euarthropod. Curr. Biol. *30*, 3057–3061.e2. https://doi.org/10.1016/j.cub.2020.05.085.
3. Tanaka, G., Hou, X., Ma, X., Edgecombe, G.D., and Strausfeld, N.J. (2013). Chelicerate neural ground pattern in a Cambrian great appendage arthropod. Nature *502*, 364–367. https://doi.org/10.1038/nature12520.
4. O'Flynn, R.J., Liu, Y., Hou, X., Mai, H., Yu, M., Zhuang, S., Williams, M., Guo, J., and Edgecombe, G.D. (2023). The early Cambrian *Kylinxia zhangi* and evolution of the arthropod head. Curr. Biol. *33*, 4006–4013.e2. https://doi.org/10.1016/j.cub.2023.08.022.
5. Siveter, D.J., Briggs, D.E.G., Siveter, D.J., Sutton, M.D., Legg, D., and Joomun, S. (2014). A Silurian short-great-appendage arthropod. Proc. Biol. Sci. *281*, 20132986. https://doi.org/10.1098/rspb.2013.2986.
6. Legg, D.A., Sutton, M.D., and Edgecombe, G.D. (2013). Arthropod fossil data increase congruence of morphological and molecular phylogenies. Nat. Commun. *4*, 2485. https://doi.org/10.1038/ncomms3485.
7. Lerosey-Aubril, R., Kimmig, J., Pates, S., Skabelund, J., Weug, A., and Ortega-Hernández, J. (2020). New exceptionally preserved panarthropods from the Drumian Wheeler Konservat-Lagerstätte of the House Range of Utah. Pap. Palaeontol. *6*, 501–531. https://doi.org/10.1002/spp2.1307.
8. Walcott, C.D. (1912). Cambrian Geology and Paleontology II. Middle Cambrian Branchiopoda, Malacostraca, Trilobita, and Merostomata. Smithsonian Misc. Coll. *57*, 145–228.
9. Edgecombe, G.D., García-Bellido, D.C., and Paterson, J.R. (2011). A new leanchoiliid megacheiran arthropod from the lower Cambrian Emu Bay Shale, South Australia. Acta Palaeontol. Polonica *56*, 385–400. https://doi.org/10.4202/app.2010.0080.
10. Simonetta, A. (1970). Studies on non trilobite arthropods of the Burgess Shale (Middle Cambrian). The genera *Leanchoilia*, *Alalcomenaeus*, *Opabinia*, *Burgessia*, *Yohoia* and *Actaeus*. Palaeontographia Italica *66*, 35–45.
11. Briggs, D.E.G., and Collins, D. (1999). The arthropod *Alalcomenaeus cambricus* Simonetta, from the Middle Cambrian Burgess Shale of British Columbia. Palaeontology *42*, 953–977. https://doi.org/10.1111/1475-4983.00104.
12. Aria, C., Caron, J.B., and Gaines, R. (2015). A large new leanchoiliid from the Burgess Shale and the influence of inapplicable states on stem arthropod phylogeny. Palaeontology *58*, 629–660. https://doi.org/10.1111/pala.12161.
13. Ortega-Hernández, J., Janssen, R., and Budd, G.E. (2017). Origin and evolution of the panarthropod head–a palaeobiological and developmental perspective. Arthropod Struct. Dev. *46*, 354–379. https://doi.org/10.1016/j.asd.2016.10.011.
14. Lankester, E.R. (1904). The structure and classification of the Arthropoda. J. Cell Sci. *S2–47*, 523–582. https://doi.org/10.1242/jcs.s2-47.188.523.
15. Hou, X., and Bergström, J. (1997). Arthropods of the lower Cambrian Chengjiang fauna, southwest China. Fossils and Strata, 1–116.
16. Størmer, L. (1944). On the relationships and phylogeny of fossil and recent Arachnomorpha: a comparative study on Arachnida, Xiphosura, Eurypterida, Tribolita, and other fossil Arthropoda. Skrifter Utgitt av Det Norske Videnskaps-Akademi i Oslo. I. Matematisk-Naturvitenskapelig Klasse *5*, 1–158.
17. Raymond, P.E. (1935). *Leanchoilia* and other mid-Cambrian Arthropoda. Bull. Mus. Comp. Zool. *76*, 205–230.
18. Farrell, U.C., Briggs, D.E.G., Hammarlund, E.U., Sperling, E.A., and Gaines, R.R. (2013). Paleoredox and pyritization of soft-bodied fossils in the Ordovician Frankfort Shale of New York. Am. J. Sci. *313*, 452–489. https://doi.org/10.2475/05.2013.02.
19. Briggs, D.E.G., Bottrell, S.H., and Raiswell, R. (1991). Pyritization of soft-bodied fossils: Beecher's Trilobite Bed, Upper Ordovician, New York State. Geology *19*, 1221–1224. https://doi.org/10.1130/0091-7613(1991)019<1221:POSBFB>2.3.CO;2.
20. Farrell, U.C., Briggs, D.E.G., and Gaines, R.R. (2011). Paleoecology of the olenid trilobite *Triarthrus*: new evidence from Beecher's Trilobite Bed and other sites of pyritization. Palaios *26*, 730–742. https://doi.org/10.2110/palo.2011.p11-050r.
21. Liu, Y., Edgecombe, G.D., Schmidt, M., Bond, A.D., Melzer, R.R., Zhai, D., Mai, H., Zhang, M., and Hou, X. (2021). Exites in Cambrian arthropods and homology of arthropod limb branches. Nat. Commun. *12*, 4619. https://doi.org/10.1038/s41467-021-24918-8.

Please cite this article in press as: Parry et al., A pyritized Ordovician leanchoiliid arthropod, Current Biology (2024), https://doi.org/10.1016/j.cub.2024.10.013

22. Mongiardino Koch, N., Garwood, R.J., and Parry, L.A. (2021). Fossils improve phylogenetic analyses of morphological characters. Proc. R. Soc. Lond. B *288*, 20210044.

23. Gabbott, S.E., Hou, X., Norry, M.J., and Siveter, D.J. (2004). Preservation of Early Cambrian animals of the Chengjiang biota. Geology *32*, 901–904. https://doi.org/10.1130/G20640.1.

24. Briggs, D.E.G., Raiswell, R., Bottrell, S.H., Hatfield, D., and Bartels, C. (1996). Controls on the pyritization of exceptionally preserved fossils; an analysis of the Lower Devonian Hunsrük Slate of Germany. Am. J. Sci. *296*, 633–663. https://doi.org/10.2475/ajs.296.6.633.

25. Van Roy, P., Orr, P.J., Botting, J.P., Muir, L.A., Vinther, J., Lefebvre, B., el Hariri, K., and Briggs, D.E.G. (2010). Ordovician faunas of Burgess Shale type. Nature *465*, 215–218. https://doi.org/10.1038/nature09038.

26. Kühl, G., Briggs, D.E.G., and Rust, J. (2009). A great-appendage arthropod with a radial mouth from the Lower Devonian Hunsruck Slate, Germany. Science *323*, 771–773. https://doi.org/10.1126/science.1166586.

27. Whittington, H.B., and Almond, J. (1987). Appendages and habits of the Upper Ordovician trilobite *Triarthrus eatoni*. Phil. Trans. R. Soc. Lond. B *317*, 1–46. https://doi.org/10.1098/rstb.1987.0046.

28. Cisne, J.L. (1981). *Triarthrus eatoni* (Trilobita); anatomy of its exoskeletal, skeletomuscular, and digestive systems. Palaeontogr. Am. *9*, 99–140.

29. Cisne, J.L. (1975). Anatomy of *Triarthrus* and the relationships of the Trilobita. Fossils and Strata *4*, 45–63.

30. Hou, J.-B., Hughes, N.C., and Hopkins, M.J. (2021). The trilobite upper limb branch is a well-developed gill. Sci. Adv. *7*, eabe7377. https://doi.org/10.1126/sciadv.abe7377.

31. Haug, J.T., Briggs, D.E.G., and Haug, C. (2012). Morphology and function in the Cambrian Burgess Shale megacheiran arthropod *Leanchoilia superlata* and the application of a descriptive matrix. BMC Evol. Biol. *12*, 162. https://doi.org/10.1186/1471-2148-12-162.

32. Zhang, X., Liu, Y., O'Flynn, R.J., Schmidt, M., Melzer, R.R., Hou, X., Mai, H., Guo, J., Yu, M., and Ortega-Hernández, J. (2022). Ventral organization of *Jianfengia multisegmentalis* Hou, and its implications for the head segmentation of megacheirans. Palaeontology *65*, e12624. https://doi.org/10.1111/pala.12624.

33. He, Y.-Y., Cong, P.-Y., Liu, Y., Edgecombe, G.D., and Hou, X. (2017). Telson morphology of Leanchoiliidae (Arthropoda: Megacheira) highlighted by a new *Leanchoilia* from the Cambrian Chengjiang biota. Alcheringa: An Australasian Journal of Palaeontology *41*, 581–589. https://doi.org/10.1080/03115518.2017.1320425.

34. Van Roy, P., Daley, A.C., and Briggs, D.E.G. (2015). Anomalocaridid trunk limb homology revealed by a giant filter-feeder with paired flaps. Nature *522*, 77–80. https://doi.org/10.1038/nature14256.

35. Aria, C. (2022). The origin and early evolution of arthropods. Biol. Rev. Camb. Philos. Soc. *97*, 1786–1809. https://doi.org/10.1111/brv.12864.

36. Struck, T.H., Haug, C., Haszprunar, G., Prpic, N.-M., and Haug, J.T. (2015). *Enalikter aphson* is more likely an annelid than an arthropod: a comment to Siveter et al. (2014). Proc. R. Soc. Lond. B *282*, 20140946.

37. Parry, L.A., Legg, D.A., and Sutton, M.D. (2017). *Enalikter* is not an annelid: homology, autapomorphies and the interpretation of problematic fossils. Lethaia *50*, 222–226. https://doi.org/10.1111/let.12196.

38. Siveter, D.J., Briggs, D.E.G., Siveter, D.J., Sutton, M.D., Legg, D., and Joomun, S. (2015). *Enalikter aphson* is an arthropod: a reply to Struck et al. (2014). Proc. R. Soc. B. *282*, 20142663. https://doi.org/10.1098/rspb.2014.2663.

39. Liu, Y., Hou, X., and Bergström, J. (2007). Chengjiang arthropod *Leanchoilia illecebrosa* (Hou, 1987) reconsidered. GFF *129*, 263–272. https://doi.org/10.1080/11035890701293263.

40. Liu, Y., Haug, J.T., Haug, C., Briggs, D.E.G., and Hou, X. (2014). A 520 million-year-old chelicerate larva. Nat. Commun. *5*, 4440. https://doi.org/10.1038/ncomms5440.

41. Aria, C., Zhao, F., Zeng, H., Guo, J., and Zhu, M. (2020). Fossils from South China redefine the ancestral euarthropod body plan. BMC Evol. Biol. *20*, 4. https://doi.org/10.1186/s12862-019-1560-7.

42. Cisne, J.L. (1973). Beecher's Trilobite Bed revisited: Ecology of an Ordovician deepwater fauna. Postilla *160*, 1–25.

43. Schmidt, M., Hou, X., Mai, H., Zhou, G., Melzer, R.R., Zhang, X., and Liu, Y. (2024). Unveiling the ventral morphology of a rare early Cambrian great appendage arthropod from the Chengjiang biota of China. BMC Biol. *22*, 96. https://doi.org/10.1186/s12915-024-01889-y.

44. Lev, O., Edgecombe, G.D., and Chipman, A.D. (2022). Serial homology and segment identity in the arthropod head. Integr. Org. Biol. *4*, obac015. https://doi.org/10.1093/iob/obac015.

45. Budd, G.E. (2002). A palaeontological solution to the arthropod head problem. Nature *417*, 271–275. https://doi.org/10.1038/417271a.

46. Lan, T., Zhao, Y., Zhao, F., He, Y., Martinez, P., and Strausfeld, N.J. (2021). Leanchoiliidae reveals the ancestral organization of the stem euarthropod brain. Curr. Biol. *31*, 4397–4404.e2. https://doi.org/10.1016/j.cub.2021.07.048.

47. Chen, J., Waloszek, D., and Maas, A. (2004). A new 'great-appendage' arthropod from the Lower Cambrian of China and homology of chelicerate chelicerae and raptorial antero-ventral appendages. Lethaia *37*, 3–20. https://doi.org/10.1080/00241160410004764.

48. Scholtz, G., and Edgecombe, G.D. (2006). The evolution of arthropod heads: reconciling morphological, developmental and palaeontological evidence. Dev. Genes Evol. *216*, 395–415. https://doi.org/10.1007/s00427-006-0085-4.

49. Aria, C., Zhao, F., and Zhu, M. (2021). Fuxianhuiids are mandibulates and share affinities with total-group Myriapoda. J. Geol. Soc. *178*, jgs2020–jgs2246. https://doi.org/10.1144/jgs2020-246.

50. Snodgrass, R.E. (1948). Textbook of Arthropod Anatomy (Cornell University Press).

51. El Albani, A., Mazurier, A., Edgecombe, G.D., Azizi, A., El Bakhouch, A., Berks, H.O., Bouougri, E.H., Chraiki, I., Donoghue, P.C.J., Fontaine, C., et al. (2024). Rapid volcanic ash entombment reveals the 3D anatomy of Cambrian trilobites. Science *384*, 1429–1435. https://doi.org/10.1126/science.adl4540.

52. Ortega-Hernández, J., and Budd, G.E. (2016). The nature of non-appendicular anterior paired projections in Palaeozoic total-group Euarthropoda. Arthropod Struct. Dev. *45*, 185–199. https://doi.org/10.1016/j.asd.2016.01.006.

53. Park, T.S. (2023). Trilobite hypostome as a fusion of anterior sclerite and labrum. Arthropod Struct. Dev. *77*, 101308. https://doi.org/10.1016/j.asd.2023.101308.

54. Van Roy, P., and Briggs, D.E.G. (2011). A giant Ordovician anomalocaridid. Nature *473*, 510–513. https://doi.org/10.1038/nature09920.

55. Vinther, J., Stein, M., Longrich, N.R., and Harper, D.A.T. (2014). A suspension-feeding anomalocarid from the Early Cambrian. Nature *507*, 496–499. https://doi.org/10.1038/nature13010.

56. Park, T.S., Nielsen, M.L., Parry, L.A., Sørensen, M.V., Lee, M., Kihm, J.-H., Ahn, I., Park, C., de Vivo, G., Smith, M.P., et al. (2024). A giant stem-group chaetognath. Sci. Adv. *10*, eadi6678. https://doi.org/10.1126/sciadv.adi6678.

57. Ronquist, F., Teslenko, M., van der Mark, P., Ayres, D.L., Darling, A., Höhna, S., Larget, B., Liu, L., Suchard, M.A., and Huelsenbeck, J.P. (2012). MrBayes 3.2: efficient Bayesian phylogenetic inference and model choice across a large model space. Syst. Biol. *61*, 539–542. https://doi.org/10.1093/sysbio/sys029.

58. Ponchio, F., Corsini, M., and Scopigno, R. (2019). RELIGHT: A compact and accurate RTI representation for the web. Graph. Models *105*, 101040. https://doi.org/10.1016/j.gmod.2019.101040.

Please cite this article in press as: Parry et al., A pyritized Ordovician leanchoiliid arthropod, Current Biology (2024), https://doi.org/10.1016/j.cub.2024.10.013

59. Zeng, H., Zhao, F., Niu, K., Zhu, M., and Huang, D. (2020). An early Cambrian euarthropod with radiodont-like raptorial appendages. Nature *588*, 101–105. https://doi.org/10.1038/s41586-020-2883-7.

60. Nixon, K. (2002). WinClada, version 1.00. 08 (published by the author, Ithaca, New York).

61. Goloboff, P.A., and Catalano, S.A. (2016). TNT version 1.5, including a full implementation of phylogenetic morphometrics. Cladistics *32*, 221–238. https://doi.org/10.1111/cla.12160.

62. Lewis, P.O. (2001). A likelihood approach to estimating phylogeny from discrete morphological character data. Syst. Biol. *50*, 913–925. https://doi.org/10.1080/106351501753462876.

Please cite this article in press as: Parry et al., A pyritized Ordovician leanchoiliid arthropod, Current Biology (2024), https://doi.org/10.1016/j.cub.2024.10.013

STAR★METHODS

KEY RESOURCES TABLE

REAGENT or RESOURCE	SOURCE	IDENTIFIER
Fossil specimens		
Lomankus edgecombei specimens	Yale Peabody Museum	YPM IP 256612, YPM IP 256613, YPM IP 236743, YPM IP 516237, YPM IP 236744.
Deposited data		
Morphological character matrix in NEXUS format	This study	Table S1
RTI datasets	This study	Oxford Research Archive: http://dx.doi.org/10.5287/ora-mnjxxmoyd
CT datasets	This Study	Oxford Research Archive: http://dx.doi.org/10.5287/ora-mnjxxmoyd
Software and algorithms		
MrBayes 3.2.7	Ronquist et al.[57]	http://nbisweden.github.io/MrBayes/
RTI Viewer	CNR-ISTI Visual Computing lab	http://vcg.isti.cnr.it/rti/rtiviewer.php
TNT 1.5	Willi Hennig Society	https://cladistics.org/tnt/

EXPERIMENTAL MODEL AND STUDY PARTICIPANT DETAILS

Fossil specimens

We studied five fossil specimens from the from the Upper Ordovician (Katian) Beecher's Trilobite Bed site of New York State that are deposited in the collections of the Yale Peabody Museum. Beecher considered the original bed mined out[42] but it was rediscovered in 1984 and excavated in 1989 and much more extensively in 2004. The 2004 excavation exposed the original 4 cm thick bed laterally through ~85 m[18] and revealed a number of other levels with pyritized soft tissues within the meter above it,[20] one of which yielded ostracods with pyritized appendages. The specimens described here were discovered more recently as a product of further collecting at the Beecher's Trilobite Bed site.

METHOD DETAILS

Reflectance transformation imaging

Reflectance transformation imaging (RTI) was used to enhance the three-dimensional surface morphology of the specimens, particularly where some of the pyrite had been lost due to preparation or during splitting. Specimens were Illuminated using a FlyDome RTI dome and images were taken with a Canon EOS 5D mkiv using a Canon EF 100 mm macro lens or a Canon MP-E 65 mm lens for higher magnification. For datasets using the Canon EF 100 mm macro lens, 54 images were taken, but the Canon MP-E 65 mm lens occluded the top row of LEDs, resulting in a dataset of 42 images. The resulting image datasets were used to make polynomial texture maps in RTI format using RelightLab[58] and were visualized using RTI viewer. The diffuse gain and normal visualization imaging modes were used to enhance topographic information. Lighting directions and visualization parameters are included in Table S1.

CT scanning and reconstruction

Specimens used in this study were scanned with an Xradia 520 Versa at Yunnan Key Laboratory for Palaeobiology (YPM IP 256612, YPM IP 256613) or with a Nikon XTek XT H225 scanner at Harvard University (YPM IP 236743, YPM IP 516237). Scanning parameters were as follows: YPM IP 256612–Beam strength 70kV/6w, no Filter, Resolution 4.89μm, Number of TIFF images 4058; YPM IP 256613–Beam strength 70kV/6w, no Filter, Resolution 4.23μm, Number of TIFF images 2554; YPM IP 236743–Beam strength 110kV/280μA, Copper filter, Resolution 7.94μm, Number of X-ray projections 3142; YPM IP 516237–Beam strength 100kV/150μA, Copper filter, Resolution 13.73μm, Number of X-ray projections 3143. YPM IP 516237–Beam strength 100kV, 0.1 mm copper filter, Resolution 13.7μm, YPM IP 236744 –Beam strength 110kV, 0.5 mm copper filter, Resolution 14.4μm. 3D visualisation methods followed those used in recent studies of arthropods from the Chengjiang Biota[32]: grayscale TIFF stacks generated by the CT scanners were loaded into Drishti-import-64 (v2.4) to generate a pair of.*pvl.nc* files that were then stacked in Drishti-64 (v2.4) and further processed with the 'Transfer Function Editor' within the software. Mopping and clipping tools were used to remove noise in the background, and to digitally dissect the structures of interest. In some cases, the 3D models were visualized with the 'Shadow Widget' activated. Clear and informative views of the 3D models were then screen-captured as images and arranged into figures.

Please cite this article in press as: Parry et al., A pyritized Ordovician leanchoiliid arthropod, Current Biology (2024), https://doi.org/10.1016/j.cub.2024.10.013

CellPress
OPEN ACCESS

QUANTIFICATION AND STATISTICAL ANALYSIS

Phylogenetic analysis

The phylogenetic position of *Lomankus edgecombei* was inferred using the data matrix of O'Flynn et al.[4] (itself modified from Zeng et al.[59]) with *L. edgecombei* and *Oestokerkus megacholix*[9] added. This matrix includes 283 characters and 87 taxa. The data matrix was constructed in WinClada 1.00.08.[60]

In contrast to *Leanchoilia illecebrosa* and *Leanchoilia superlata*, *Lomankus edgecombei* exhibits the following character states (numbered as in Zeng et al.[59]): (1) eyes (char. 18) absent; (2) compound eyes (char. 20) absent; (3) median eyes (char. 29) absent; (4) anteriormost sclerite associated with eyes (char. 65) absent; (5) orientation of pleurae (char. 123) pleurae around body (i.e., character state 1 in Zeng et al.[59]); (6) telson fringed with setae (char. 140) absent; (7) frontalmost appendages, endites well-developed, raptorial (char. 179) absent; (8) frontalmost appendages, terminal claw bearing multiple cusps (char. 180) similar to other podomeres; (9) frontalmost appendages (arthropodized), number of podomeres bearing well-expanded endites, terminal podomere excluded (char. 188) 0 or 1 (character state 0); (10) frontalmost appendages (arthropodized), differentiated main spines or main protrusions of endites (char. 190) absent; (11) frontalmost appendages (arthropodized), elongate terminal podomere (char. 206) absent; (12) frontalmost appendages (arthropodized), length of flagella (char. 208) midlength of trunk; (13) frontalmost appendages (arthropodized), raptorial device made of three to four podomeres with elongated endites (char. 211) absent; (14) anterior reduction of segments and/or appendages (char. 219) present; (15) specialized post-antennal appendages (SPAs) (char. 221) present; (16) morphology of appendages on third head segment (char. 222) heteronomous to posterior appendages, or reduced, forming intercalary segment (character state 1); (17) number of unique morphological types of anteriormost appendage pairs (char. 227) 2; (18) post-oral appendages, endopodite, number of podomeres with distal claw included (char. 252) equal to or fewer than 6; and (19) number of post-frontal appendages (post-FA) pairs (char. 283) 11-14.

In contrast to *Leanchoilia illecebrosa* and *Leanchoilia superlata*, *Oestokerkus megacholix* exhibits: (1) median eyes (char. 29) absent; (2) additional anterior marginal structures of head shield (char. 96) absent; (3) orientation of pleurae (char. 123) pleurae around body (character state 1); (4) frontalmost appendages (arthropodized), length of flagella (char. 208) midlength of trunk; and (5) anterior homonomous appendages in head smaller, differentiated in size from posterior ones (char. 218) absent.

Based on new data (cf. O'Flynn et al.[4] for context), we recoded the following character in *Priapulus caudatus*, *Cricocosmia jinningensis*, Tardigrada, *Microdictyon sinicum*, *Paucipodia inermis*, *Cardiodictyon catenulum*, *Hallucigenis fortis*, *Collinsium ciliosum*, *Luolishania longicruris*, *Onychodictyon ferox*, *Aysheaia pedunculata*, *Antennacanthopodia gracilis*, Onychophora, *Megadictyon haikoucaris*, *Pambdelurion whittingtoni*, *Kerygmachela kierkegaardi*: exite (modified from epipodite — see Zeng et al.,[59] char. 279 for context) from inapplicable to absent. We also recoded char. 279 from absent to present in *Leanchoilia illecebrosa*, *Retifacies abnormalis* and *Naraoia spinosa*, and from absent to unknown in *Leanchoilia superlata*, *Tegopelte gigas*, *Helmetia expansa* and *Kuamaia lata*.

Maximum parsimony analyses were performed with Tree analysis using New Technology (TNT) 1.5.[61] All characters were treated as unordered. The software was set to retain 99,999 trees and perform 10,000 replications. Each analysis included a traditional search with tree bisection and reconnection, a random seed of 1, and 1000 trees were saved per replicate. Jackknife supports (under equal weights), and group present/contradicted (GC) frequency differences (under implied weights) of nodes on the trees were calculated by resampling using 1000 replicates of traditional search, with a change probability of 36% and 33%, respectively, for the two types of nodal supports.

Bayesian analyses used MrBayes 3.2.7[57] employing the mki + gamma model, correcting for ascertainment bias from the coding of parsimony informative characters alone.[62] 100,000,000 generations were requested, and analyses ceased once the average deviation of split frequencies was <0.01. Convergence was further assessed using PSRF (~1.0) and Effective Sample Sizes (>200) using the sump command. Analyses stopped after 1790000 generations. Parameters and consensus trees were summarized with a burn-in fraction of 0.25.